Utilization of Municipal Wastewater for Cooling in Thermoelectric Power Plants

Iman Safari[a], Michael E. Walker[a], Ming-Kai Hsieh[b], David A. Dzombak[b],Wenshi Liu[c], Radisav D. Vidic[c], David C. Miller[d], and Javad Abbasian[a*]

[a]Illinois Institute of Technology, Chicago, Illinois
[b]Carnegie Mellon University, Pittsburgh, Pennsylvania
[c]University of Pittsburgh, Pittsburgh, Pennsylvania
[d]National Energy Technology Laboratory, Morgantown, West Virginia

Abstract

A process simulation model has been developed using Aspen Plus® with the OLI (OLI System, Inc.) water chemistry model to predict water quality in the recirculating cooling loop utilizing secondary- and tertiary-treated municipal wastewater as the source of makeup water. Simulation results were compared with pilot-scale experimental data on makeup water alkalinity, loop pH, and ammonia evaporation. The effects of various parameters including makeup water quality, salt formation, NH_3 and CO_2 evaporation mass transfer coefficients, heat load, and operating temperatures were investigated. The results indicate that, although the simulation model can capture the general trends in the loop pH, experimental data on the rates of salt precipitation in the system are needed for more accurate prediction of the loop pH. It was also found that stripping of ammonia and carbon dioxide in the cooling tower can influence the cooling loop pH significantly. The effects of the NH_3 mass transfer coefficient on cooling loop pH appear to be more significant at lower values (e.g., $k_{NH3} < 4\times10^{-3}$ m/s) when the makeup water alkalinity is low (e.g., <90 mg/L as $CaCO_3$). The effect of the CO_2 mass transfer coefficient was found to be significant only at lower alkalinity values (e.g., $k_{CO2}<4\times10^{-6}$ m/s).

Keywords: Municipal Wastewater; Cooling System; Thermoelectric Power plant; Water Chemistry; Water Quality; Modeling; Simulation; Cooling Tower

Introduction

Thermoelectric power production in the United States uses a large amount of freshwater. The industry withdrew 143 BGD in 2005, accounting for about 41% of total freshwater withdrawal (USGS, 2009). The total amount of freshwater consumed by the industry in 1995 was 3.3 BGD, accounting for 3.3% of all freshwater consumption (USGS, 1998). This large water demand is increasingly a problem, especially for new power plant development, as availability of freshwater for new uses diminishes in the U.S. (USGAO, 2003). Use of non-traditional water sources, such as secondary-treated municipal wastewater (MWW), provides one option to reduce freshwater usage in thermoelectric power production (Li et al., 2011a). Utilization of MWW in cooling systems requires careful management of water quality in the cooling system because of the increased potential for mineral precipitation on heat exchanger surfaces (Li et al., 2011b).

The accumulation of deposits on the surfaces of heat exchangers is usually referred to as fouling (Bott, 1995), which can include both mineral deposition (scaling) and biofouling. In thermoelectric power plant cooling systems, fouling lowers the overall heat transfer coefficient and negatively impacts power production efficiency (Walker et al, 2012).

Much work has been done to identify the important parameters affecting fouling and to quantify their impacts (Li et al., 2011b; Hawthorn, 2009; Nebot et al., 2007; Sultan et al., 1996; Hasson et al., 1978; Taborek et al., 1972a; Taborek et al., 1972b). The parameters considered in these studies include hydrodynamics characteristics inside the condenser tubes, surface temperature, tube properties, and water quality. Among these parameters, water quality characteristics are of greatest importance when MWW, which has higher concentrations of fouling components, is used in the cooling system (DOE/NETL, 2009a; DOE/NETL, 2009b; Argonne National Laboratory, 2007; EPRI, 2003).

Although several studies have investigated the effect of recirculating loop water quality on fouling rate, the relationship between the properties of the makeup water and the loop water has not been addressed (Hawthorn, 2009; Ning, 2002; Morse & Knudsen, 1977; Hasson et al., 1968a). The most important parameters that affect the loop water properties include the makeup water characteristics, cycles of concentrations (COC), release of volatile constituents in the cooling tower, and formation/ deposition of salts in the system.

This paper presents a process model for predicting water quality in the cooling loop as a function of operating parameters and the makeup water quality. The model will be useful for evaluating the potential performance and treatment needs for alternative sources of cooling water, such as MWW. In addition, the model can be used to assess the economic impact of municipal wastewater utilization in the thermoelectric power plants (Walker et al., 2012).

Recirculating Cooling System

A schematic diagram of a typical recirculating cooling system is shown in Figure 1a, which includes an optional makeup water treatment subsystem and the cooling loop, including the cooling tower and the condenser. The makeup water entering the recirculating cooling loop is concentrated about 3 to 10 times depending on the cycle of concentration (COC) of the process (EPRI, 2003):

$$(COC) = \frac{C_{i,L}}{C_{i,MU}} \quad (1)$$

Where, $C_{i,MU}$ and $C_{i,L}$ are the concentration of the constituent i in the makeup and recirculating loop, respectively.

In a cooling loop, volatile species such as CO_2 and NH_3 are stripped, to varying extents, from the water in the cooling tower, changing the total carbonate and ammonia concentration of the aqueous phase, while formation of the salts such as calcium carbonate and their deposition on heat transfer surfaces reduces the concentration of the associated species in the water. Both the cooling tower and the condenser affect the water chemistry through the formation of salts, and in the cooling tower there also is evaporation of volatile constituents.

Water Chemistry

Determination of the interrelated effects of makeup water quality, deposition of the salt in the condenser, release of volatiles in the cooling tower, and the cycles of concentration on the water quality in the cooling loop requires a comprehensive chemical speciation analysis in the aqueous phase. In general, it is reasonable to assume that the reactions among dissolved species in the aqueous phase are sufficiently fast to achieve equilibrium.

Although several studies have examined the effect of carbonate concentration on fouling (Segev et al., 2012; Wiechers, 1975; Hasson et al., 1968b), a more comprehensive water chemistry consideration with a broad range of species expected in degraded waters is required to properly predict the properties of the water in the recirculating cooling loop since degraded waters have much higher concentrations of non-carbonate species such as ammonia, phosphate, and sulfates. Given the very large number (i.e., >100) of components and reactions to be considered for the aqueous phase, a software with a comprehensive thermodynamic equilibrium package is needed to carry out energy and mass balances in the entire system. In this study, Aspen Plus® software was used for energy and mass balances calculations, along with the OLI thermodynamic package (OLI System, Inc.) for detailed water chemistry speciation.

Water Treatment Subsystems

MWW generally requires additional, tertiary treatment to achieve a quality consistent with manageable scaling, biofouling, and corrosion (Bott, 1995; Hsieh et al., 2010; Li et al., 2011b). The average properties of a typical secondary-treated municipal wastewater are presented in Table 1. The cooling system makeup water treatment subsystem for tertiary treatment of MWW may consist of several separate unit operations such as filtration to remove suspended solids, softening to remove hardness, nitrification to remove ammonia, and acid addition to adjust the pH of the water. In all cases considered in this study, it was assumed that all suspended solids had already been removed by filtration. The nitrification process was simulated in Aspen Plus® with OLI chemistry as an activated sludge process to estimate the properties of nitrified secondary-treated municipal wastewater (MWW-N). It should be noted that bicarbonate can be added during the nitrification process to maintain the desired level of pH and/or alkalinity. The simulated composition of MWW-N is also presented in Table 1, indicating that more than 95% of ammonia is removed, resulting in significant consumption of the alkalinity and reduction in the pH of the nitrified water. Acidification simply involves addition of an acid to control the pH of the water. In this study, H_2SO_4 was selected for the acidification process.

Cooling Tower

Modeling and simulation of a cooling tower generally involves simultaneously solving a large number of mass and heat transfer equations for a multicomponent system. However, given the relatively low concentration of the components dissolved in the water, the liquid phase can be treated as pure water to determine the rate of water evaporation as well as the air flow rate through the cooling tower. The calculated values of the water evaporation and air flow rates can

then be used to obtain the rate of vaporization of volatile components from the cooling tower and to perform aqueous phase speciation.

Different approaches and models have been proposed to estimate the rate of water evaporation and air flow rate in a cooling tower where the liquid phase is represented by pure water (Williamson, 2008; Kröger, 2004; Kloppers & Kröger, 2001; Kröger, 1998; Poppe, 1991; Merkel, 1925). Among these methods, the widely-used model proposed by Merkel (Merkel, 1925) was selected to simulate the cooling tower performance. This method simplifies the one-dimensional heat and mass transfer equations by assuming constant water flow rate in the cooling tower and saturated air leaving the tower. It has been shown that the results predicted by the Merkel method are sufficiently accurate for practical applications (Kröger, 2004; Kloppers & Kröger, 2001; Kröger, 1998). The enthalpy and the mass flow rate of the air leaving the tower are determined from the following coupled equations:

$$\frac{dH_a}{dT^w} = \frac{m_w}{m_a} Cp_w \tag{2}$$

$$M_e = \int_{T^{wo}}^{T^{wi}} \frac{Cp_w dT^w}{(H_a{}^{T^w} - H_a)} \tag{3}$$

$$M_e = \frac{KA}{m_w} = \frac{K(aA_{fr}L)}{m_w} = \frac{KaL}{G_w} \tag{4}$$

where H_a is the enthalpy of air and $H_a{}^{T^w}$ is enthalpy of saturated air evaluated at the water temperature, T^w is the water temperature, Cp_w is the heat capacity of the water, and m_w and m_a represent the mass flow rates of water and air, respectively. In Equations 3 and 4 M_e is the Merkel number, T^{wi} and T^{wo} are the water temperatures at the inlet and outlet of the cooling

tower, K is the mass transfer coefficient, G_w is the specific mass flow rate of the water, while A, a, A_{fr}, and L are the mass transfer area, the specific area, the frontal area, and the length of the tower, respectively. The rate of water evaporation is calculated based on the mass flow rate and enthalpy of the air, assuming the air is saturated at the outlet of the cooling tower.

The mass and heat transfer coefficients, as well as the specific area of the tower, are usually reported in terms of the Merkel number for different zones of the tower. In general, there are three different mass and heat transfer zones in the cooling tower as shown in Figure 1b (Kröger, 1998). The first zone (i.e., spray zone) uniformly distributes the water to the top of the fill zone through the nozzles. Most of the heat and mass transfer takes place in the fill zone and water enters the rain zone in the form of droplets and is collected in the cooling tower sump and pumped back to the condenser. The Merkel numbers for the different zones of the cooling tower can be calculated using correlations available in the literature. It has been shown that the rain and spray zones can contribute to up to 30% and 5% of the overall heat removal in a typical cooling tower, respectively (Kröger, 2004). For example, the Merkel number for the fill zone can be calculated by the following correlation (Kloppers, 2003):

$$M_{e-fz} = n_1 L_{fz} (G_w)^{n_2} (G_a)^{n_3} \quad (5)$$

where M_{e-fz} is the Merkel number of the fill zone, L_{fz} is the height of the fill zone, G_a is the specific mass flow of the air, while n_1, n_2, and n_3 are the correlation parameters. Although the water evaporation rate in the cooling tower can be obtained by solving Equations 2 to 5 to predict the water evaporation rate as well as the water flow rate through the cooling loop, these equations should be simultaneously solved with the material and energy balance equations for

the entire loop using an iterative scheme. The water evaporation rate, makeup, and blowdown flow rates are related through the following mass balance equations:

$$(COC) = \frac{F_{MU}}{F_B} = 1 + \frac{F_E}{F_B} \tag{6}$$

where F_{MU}, F_B, and F_E are the volumetric flow rate of makeup, blowdown, and evaporation, respectively.

When the water evaporation rate and the air flow rate are determined, the rate of evaporation of volatile species (mainly NH_3 and CO_2) are determined based on the mass transfer limitation and/or the chemical equilibria of the following reactions:

$$NH_4^+ \rightleftarrows NH_3 + H^+ \tag{A}$$

$$HCO_3^- + H^+ \rightleftarrows H_2O + CO_2 \tag{B}$$

The rate of evaporation of volatile species in the cooling tower can be expressed as (Hsieh et al., 2012):

$$N_{NH_3} = \int_0^L k_{NH_3} \cdot a \cdot A_{fr} \cdot (C_{NH_3,air}{}^* - C_{NH_3,air}) \cdot dz \tag{7}$$

where N_{NH3} is the rate of evaporation of ammonia, k_{NH3} is the overall mass transfer coefficient based on the gas phase, $C_{NH3,air}$ is the concentration of ammonia in the air, and $C_{NH3,air}{}^*$ is the ammonia concentration in gas phase in equilibrium with the aqueous phase which can is obtained from the following equation:

$$C_{NH_3,air}^{*} = \frac{C_{NH_3}}{(KH)_{NH_3}} \quad (8)$$

where C_{NH3} is the concentration of NH_3 in the aqueous phase and $(KH)_{NH3}$ is the Henry's constant for NH_3. A similar expression can be obtained for CO_2 using the driving force in the aqueous phase:

$$N_{CO_2} = \int_0^L k_{CO_2} \cdot a \cdot A_{fr} \cdot (C_{CO_2} - C_{CO_2}^{*}) \cdot dz \quad (9)$$

where N_{CO2} is the rate of evaporation of carbon dioxide, k_{CO2} is the overall mass transfer coefficient based on aqueous phase, C_{CO2} is the concentration CO_2 in aqueous phase, and C_{CO2}^{*} is the concentration in aqueous phase in equilibrium with the gas phase, obtained from the following equation:

$$C_{CO_2}^{*} = C_{CO_2,air} \cdot (KH)_{CO_2} \quad (10)$$

where $C_{CO2,air}$ is the concentration of CO_2 in the air and $(KH)_{CO2}$ is the Henry's constant for CO_2. the Henry's constant for ammonia and carbon dioxide can be expressed as (Sander, 1999):

$$(KH)_{NH3} = 60\mathrm{Exp}\left[4100\left(\frac{1}{T_{avg}} - \frac{1}{298.15}\right)\right] \quad (11)$$

$$(KH)_{CO_2} = 0.034\mathrm{Exp}\left[2400\left(\frac{1}{T_{avg}} - \frac{1}{298.15}\right)\right] \quad (12)$$

Equations 7 to 12 are solved along the height of the tower to obtain the overall evaporation rate of volatiles in the cooling tower.

Although some information related to mass and heat transfer of pure water and air in the cooling towers has been reported in the literature (Kröger, 2004; Kloppers, 2003), the information related to the evaporation of volatile species such as NH_3 and CO_2 has been limited to that obtained in stripping towers and packed bed columns (Ma´ckowiak & Górak, 2011; Yoon, 2008; Budzianowski & Koziol, 2005; Cabassud, 2001; Sherwood et al., 1937).

Using data from experiments with pilot-scale cooling towers and MWW as makeup water (Vidic & Dzombak, D.A., 2009), Hsieh et al. (Hsieh et al., 2012) evaluated NH_3 and CO_2 removal rates and found that ammonia stripping was controlled by the gas film resistance. Based on the experimental data, Hsieh et al., (Hsieh et al., 2012) estimated the ammonia mass transfer coefficient at:

$$k_{NH3} \approx k_{NH3\text{-}g} = 2.3\times10^{-3}\ (\text{m/s}) \tag{13}$$

Safari et al. (2013) found that mass transfer coefficients for CO_2 evaporation were controlled by the mass transfer resistances in both the aqueous and gas phases and expressed the overall mass transfer coefficient, k_{CO2}, as a function of pH to represent the co-diffusion effect of bicarbonate ions:

$$\frac{1}{k_{CO_2}} = \frac{1}{k_{CO_2-g}(KH)_{CO_2}} + \frac{1}{k_{CO_2-w}\left(1+\frac{Ka1_C}{[H^+]}\right)} \tag{14}$$

where $Ka1_C$ is the first dissociation constant of carbonic acid evaluated at average air and water temperature, $[H^+]$ is the molar concentration of H^+ ions in the aqueous phase, while $k_{CO2\text{-}g}$ and $k_{CO2\text{-}w}$ are the mass transfer coefficients of CO_2 in the gas and liquid phases, respectively. From

analysis of the pilot-scale experimental data, the following values for the CO_2 gas and liquid mass transfer coefficients were estimated (Safari et al., 2013):

$$k_{CO2\text{-}g}=8\times10^{-6}\ (m/s) \quad (15)$$

$$k_{CO2\text{-}w}=8\times10^{-8}\ (m/s) \quad (16)$$

Given that no information is available for the mass transfer coefficients of volatile species and their contribution to the mass transfer of volatile species in the rain zone and spray zones of a typical cooling tower is not known, only the mass transfer in the fill zone was considered in this study. These mass transfer coefficients were used in the cooling system simulation to predict the rate of CO_2 and NH_3 evaporation in the tower and, consequently, the pH of the cooling loop.

Although formation of salts in secondary-treated municipal wastewaters containing carbonates as well as phosphate, mainly, calcium carbonate and calcium phosphate (Li et al., 2011b), can significantly impact speciation of the aqueous phase, no information is available in the literature addressing the kinetics of salt formation in such waters. Therefore, in this study, we considered the two limiting cases where, in the first case, salt formation was prevented, while, in the second case, the extent of salt formation was dictated by chemical equilibria.

Pilot-Scale Test Data

Experimental data were obtained from a pilot cooling tower operated at Franklin Township Municipal Sanitary Authority, FTMSA (Murrysville, PA) in 2010 (Dzombak et al., in preparation) that included monitoring of the loop pH at various cycles of concentration for both the secondary-treated municipal wastewater (MWW) and nitrified wastewater (MWW-N), as well ammonia monitoring for MWW.

Figure 2 shows the extent of ammonia stripping as a function of pH and cycles of concentrations (COC) in the pilot testing, indicating that the ammonia stripping efficiency was a strong function of the pH in the cooling loop.

Cooling loop water pH as a function of alkalinity of the makeup water at different cycles of concentrations for the nitrified wastewater (MWW-N) is presented in Figure 3. The results indicate that the pH of the cooling loop generally increased with the alkalinity of the makeup water, and that the pH of the loop apparently was not dependent on the COC.

Results and Discussion

Comparison of Model Simulations with Pilot-Scale Test Data

Relevant operating parameters for the cooling loop are presented in Table 1. In the model, these parameters were used in the Merkel method to calculate the outlet air temperature and humidity, the water evaporation rate, and the makeup and blowdown flow rates for different cycles of concentrations.

Figure 4 provides a comparison of the experimental data on the extent of ammonia stripping in the pilot-scale cooling tower tests for MWW (Dzombak et al., in preparation) with those predicted by the simulation model. The results predicted by the simulation model are in good agreement with the experimental data. In these simulations, MWW was acidified with H_2SO_4 to achieve the desired pH levels.

To evaluate the effect of salt formation on the extent of ammonia stripping in the cooling towers, simulation was carried out for two limiting cases: in the first case, salt precipitation was completely suppressed; in the second case, salt precipitation was dictated by chemical equilibria.

The results clearly indicate that salt formation does not have any significant impact on the ammonia stripping in the cooling tower, mainly because ammonia evaporation is a strong function of pH. Furthermore, the results also show that the rate of ammonia evaporation significantly increases as the pH of the water increases above a level of 7.

Figure 5 presents a comparison of the experimental data and model predictions of the loop pH for the nitrified secondary water (MWW-N) as a function of alkalinity of the makeup water at different cycles of concentrations. In the simulation model, the desired makeup water alkalinity was achieved by adjusting the $NaHCO_3$ content of the makeup water.

The results indicate that salt formation has a significant impact on the loop pH for MWW-N. Compared to the experimental data, higher values of pH are predicted when salt precipitation is suppressed in the model, while lower values are predicted when the extent of salt formation is dictated by chemical equilibria. In the case with no salt precipitation, the pH monotonically increases with decreasing slope, reaching an asymptotic value at high alkalinity (e.g., >50 mg/L as $CaCO_3$) for all cycles of concentrations. The initial slope is not as steep as expected for pure water because of alkalinity contributions by non-carbonate components. The asymptotic pH values predicted by the model are higher than 8.3, the pH for a mixture of pure water and $NaHCO_3$, due to the presence of non-carbonate components in the system. Additionally, in the case that is dictated by equilibrium salt formation, the results indicate an inflection point around pH 6.2, near the pKa for the first dissociation of carbonic acid. The changes in the slopes of the curves correspond to the predicted formation of various salts such as carbonate, phosphates, and silicate via chemical reaction equilibria in the system. These results indicate that although the simulation model can capture the general trends of the loop pH as a function of makeup water

alkalinity and COC, experimental data on the rates of salt precipitation in the system are needed to predict accurately the cooling loop pH.

Effect of NH_3 and CO_2 Evaporation Mass Transfer

A sensitivity analysis was performed to assess the dependence of the cooling loop water quality on the mass transfer coefficients for evaporation of NH_3 and CO_2. As the mass transfer coefficients for ammonia stripping in various unit operations have been reported to be in the range of 0.0008 to 0.01 m/s (Yoon, 2008), this range was selected to investigate the effect of the ammonia mass transfer coefficient on the cooling loop pH. The results at two levels of alkalinity are presented in Figures 6 and 7. These results indicate that, while the loop pH is not sensitive to the mass transfer coefficient of ammonia at high alkalinity levels, it can be significantly affected at low levels of alkalinity with the mass transfer coefficient below 4×10^{-3} m/s. The results also indicate that the rate of ammonia evaporation increases with increasing mass transfer coefficient, while the rate of CO_2 evaporation exhibits the reverse trend. As expressed by Equation 14, this is because the mass transfer coefficient of CO_2 decreases with decreasing pH of the solution. The combined effect of higher NH_3 and lower CO_2 evaporation results in decreasing pH of the loop with increasing ammonia mass transfer coefficient. However, at higher levels of alkalinity, because of the high buffering capacity, the pH of the solution is not affected by the rate of evaporation of CO_2 and NH_3, while, at the lower alkalinity, any slight changes in the ammonia evaporation rate can significantly affect the loop pH. Therefore, it can be concluded that at low alkalinity levels, reliable information regarding the mass transfer coefficient of ammonia is needed to predict accurately the cooling loop pH.

A similar analysis was performed to determine the sensitivity of the loop pH to the CO_2 mass transfer coefficient over the wide range of values reported in the literature (Contreras, 2007; Sherwood et al., 1937). Figures 8 and 9 show the dependence of the cooling loop water quality on the CO_2 mass transfer coefficient at different cycles of concentrations and alkalinity levels. The results indicate that the cooling loop pH is less sensitive to the mass transfer coefficient of CO_2 at lower alkalinity, but it can be significantly affected when CO_2 mass transfer coefficient is low (e.g., $k_{CO2} < 4\times10^{-6}$m/s). The results also indicate that both NH_3 and CO_2 evaporation rates increase with an increasing CO_2 mass transfer coefficient. The combined effect of higher NH_3 and CO_2 evaporation results in increasing pH of the loop with increasing CO_2 mass transfer coefficient. Therefore, it can be concluded that, to predict accurately the loop pH at high alkalinity levels, it is necessary to obtain reliable values of the CO_2 mass transfer coefficient.

Effects of Operating Parameters

The effects of several operating parameters on loop water quality were investigated by simulating different scenarios. In the baseline scenario, the cooling water temperatures at the inlet and outlet of the condenser were selected to be 35 ºC and 45 ºC, respectively; the condenser duty was assumed to be 811 MW (corresponding to a 500 MW power plant), and the cooling air inlet temperature and relative humidity were selected to be 30 ºC and 66.5 %, respectively. MWW was used as the makeup water, and considered to be at COC4.

Figure 10a shows the effect of condenser duty on the evaporation rate of volatile components as well as the pH of the cooling loop. In these calculations, it was assumed that the condenser inlet and outlet temperatures were at the baseline condition, while the water flow rate through the loop was adjusted to achieve the desired heat duty. Since COC was maintained at a constant value, the

ratios of water evaporation rates, water makeup flow rates, and blowdown flow rates were the same as the ratio of the heat duties. The results indicate that both NH_3 and CO_2 evaporation rates increase with an increase in condenser heat duty, but at a slightly lower ratio than that of the condenser duties. The combined effects of higher CO_2 and higher NH_3 evaporation rates result in a decrease in the loop pH. The lower ratio of evaporation rates can be attributed to mass transfer limitation since the mass transfer area was maintained at the baseline condition, while the cooling load of the tower was increased.

The lower ratios of evaporation rates compared to the heat duties can also be explained by estimating the evaporation rates of NH_3 and CO_2 through simplifications of the governing equations. As NH_3 and CO_2 are stripped from the tower, they are continuously replenished in the aqueous phase according to Reactions A and B. The assumption of chemical equilibrium in the aqueous phase leads to the conclusion that the concentrations of free CO_2 and NH_3 in the aqueous phase are relatively constant, while the total carbonate and ammonia contents of the recirculating water decrease as the volatile species are released. Additionally, given the very high flow rate of the air, concentrations of CO_2 and NH_3 in the air can be assumed to remain relatively constant throughout the tower. Based on these assumptions, Equations 7 and 9 can be simplified as:

$$N_{NH_3} = k_{NH3} \cdot a \cdot A_{fr} \cdot \left(\frac{C_{NH_3}}{(KH)_{NH_3}} - C_{NH_3,air}\right) \cdot L \tag{17}$$

$$N_{CO_2} = k_{CO_2} \cdot a \cdot A_{fr} \cdot (C_{CO_2} - C_{CO_2}^{*}) \cdot L \tag{18}$$

Assuming negligible concentration of ammonia in the air, Equation 17 can be further simplified:

$$N_{NH_3} = k_{NH_3} \cdot A \cdot \left(\frac{C_{NH_3}}{(KH)_{NH_3}}\right) \quad (19)$$

where A is the available area for mass transfer:

$$A = a \cdot A_{fr} \cdot L \quad (20)$$

The mass balance equation for ammonia in the cooling loop can be expressed by the following equation:

$$N_{NH_3} = (COC \cdot C_{N,MU} - C_{N,L}) \cdot F_B \quad (21)$$

where $C_{N,MU}$ and $C_{N,L}$ are the total ammonia concentration (volatile and nonvolatile forms) in the makeup and recirculating loop, respectively. Volatile fraction of the total ammonia, α, is defined as:

$$\alpha = \frac{C_{NH3}}{C_{N,L}} = f(T, pH) \quad (22)$$

which is obtained from the water chemistry calculations. Combining Equations 19 to 22 yields:

$$N_{NH3} = COC \cdot C_{N,MU} \cdot F_B \cdot \left(\frac{B_{NH_3}}{F_B + B_{NH_3}}\right) \quad (23)$$

where B_{NH3} is defined by the following equation:

$$B_{NH_3} = \frac{k_{NH_3} \cdot A \cdot \alpha}{(KH)_{NH_3}} \quad (24)$$

A similar expression can also be obtained for the CO_2 evaporation rate.

$$N_{CO_2} = \frac{COC \cdot C_{C,MU} \cdot F_B \cdot B1_{CO_2} + B1_{CO_2} \cdot B2_{CO_2}}{F_B + B1_{CO_2}} - B2_{CO_2} \quad (25)$$

where $C_{C,MU}$ is the total carbonate concentration in the makeup water and $B1_{CO2}$ and $B2_{CO2}$ are defined by the following equations:

$$B1_{CO_2} = k_{CO_2} \cdot A \cdot \beta \quad (26)$$

$$B2_{CO_2} = k_{CO_2} \cdot A \cdot (KH)_{CO_2} \cdot C_{CO_2,air} \quad (27)$$

In the above equations, β is the volatile fraction of total carbonate ($C_{C,L}$) in the recirculating cooling loop, which is obtained from the water chemistry calculations.

$$\beta = \frac{C_{CO_2}}{C_{C,L}} = f(T, pH) \quad (28)$$

Simplified expressions obtained for CO_2 and NH_3 evaporation in Equations 23 and 25 can be used to interpret the results of the simulation. The ratio of NH_3 evaporation to that of the base case is:

$$\frac{N_{NH_3}}{(N_{NH_3})_{Base}} = \left[\frac{F_B}{(F_B)_{Base}}\right] \cdot \left[\frac{B_{NH3}}{(B_{NH3})_{Base}} \cdot \frac{(F_B + B_{NH3})_{Base}}{F_B + B_{NH3}}\right] \quad (29)$$

In this equation, the first term on the right-hand side (i.e., blowdown ratio) is identical to the ratio of heat duty, while the second term is smaller than 1. Therefore, the ratio of ammonia evaporation rate is somewhat lower than the blowdown ratio. A similar analysis can be performed to estimate the ratio of CO_2 evaporation to that of a base case using Equation 25.

Figure 10b shows the effect of condenser duty on the evaporation rate of volatile components as well as the pH of the cooling loop when all operating parameters (including recirculating water flow rate) except the cooling tower inlet temperature were kept at the baseline condition. The results indicate that, similar to the previous case, both the NH_3 and CO_2 evaporation rates increase with an increase in condenser heat duty. Similarly, the combined effect of higher CO_2 and higher NH_3 evaporation results in a decrease in the cooling loop pH and the lower ratio of evaporation rates can be attributed to mass transfer limitation. Since the differences in the temperature and pH are similar to those in the previous case, the ratios of the CO_2 and NH_3 evaporation rates (and therefore the cooling loop pH) are similar to those in the previous case.

Figure 10c shows the effect of cooling range on the evaporation of the volatile species, as well as the pH of the cooling loop, where the condenser heat duty was maintained at the baseline condition, while the recirculating water flow rate was adjusted to achieve the desired water temperature at the inlet of the cooling tower. In this scenario, because of the higher contribution of the sensible heat, the rate of evaporation of water (and, therefore, the rate of blowdown) slightly decreases with increasing water temperature. Therefore, although higher inlet water temperature increases the driving force for CO_2 and NH_3 evaporation, the lower flow rates of the blowdown stream offset the increase in the evaporation rates (see Equations 23 and 25), resulting in relatively constant NH_3 and CO_2 evaporation rates as well as the pH of the loop.

Impact of Water Chemistry

The water chemistry can be simplified by limiting the species in the water to NH_3, NH_4^+, CO_2, HCO_3^-, and CO_3^{2-}. The values of the volatile fractions α and β can then be estimated using the following equations:

386 $$\alpha = \left(1 + \frac{[H^+]}{Ka_N}\right)^{-1} \quad (30)$$

387 $$\beta = \frac{1}{(1 + \frac{Ka1_C}{[H^+]} + \frac{Ka1_C \cdot Ka2_C}{[H^+]^2})} \quad (31)$$

388 Where, Ka_N is the equilibrium constant of the Reaction A and $Ka1_c$ and $Ka2_c$ are the dissociation
389 constants of carbonic acid. Figure 11a compares the values α and β obtained from OLI water
390 chemistry (OLI System, Inc.) and those obtained from Equations 30 and 31 over a wide range of
391 pH levels. The results indicate that while α can be accurately estimated with the simplified water
392 chemistry, the values of β are consistently underestimated over the entire range of pH, and the
393 relative error increases with increasing pH and can reach more than 60%.

394 Figure 11b shows the evaporation rates of both NH_3 and CO_2 predicted by the Aspen/OLI
395 simulation. The rate of evaporation of CO_2 is dictated by both the mass transfer coefficient and
396 the equilibrium concentration of CO_2 in the aqueous phase (see Equation 9). While the mass
397 transfer coefficient increases with increasing pH (see Equation 14), as shown in Figure 11a, the
398 availability of CO_2 for evaporation decreases with increasing pH. Because of these opposing
399 factors, the rate of CO_2 evaporation goes through a maximum at pH levels around 7.5.

400 The results predicted using the simplified water chemistry are also presented in Figure 11b.
401 Comparison of the results obtained with the two models indicates that the simplified model can
402 predict the evaporation rate of ammonia over a wide range of pH. The excellent agreement
403 between the two models is directly related to the similar values of α obtained from the
404 Aspen/OLI and the simplified water chemistry model. However, because of the lower β values
405 obtained from the simplified water chemistry, the rate of evaporation of CO_2 predicted by the

simple model is consistently lower than the rate predicted by the Aspen/OLI simulation. Furthermore, the lower β offsets the effect of the higher CO_2 mass transfer coefficient, resulting in a significantly lower evaporation rate compared to the rate predicted by the Aspen/OLI simulation at higher pH values, which represents the operating range of the cooling towers.

Conclusions

A process model was developed using Aspen/OLI software to simulate cooling loop water quality when secondary-treated municipal wastewater is used as makeup water. The model was tested against data from pilot-scale cooling tower experiments conducted with secondary-treated wastewater.

Results indicate that ammonia and carbon dioxide stripping in the cooling tower can influence cooling loop water quality. The simulation model can be used to estimate the extent of ammonia evaporation in the cooling tower with reasonable accuracy. The results indicate that salt formation has a significant impact on the loop pH for MWW-N. Compared to the experimental data, higher values of pH are predicted when salt precipitation is suppressed in the model, while lower values are predicted when the extent of salt formation is dictated by chemical equilibria.

The results of sensitivity analyses on the effects of NH_3 and CO_2 mass transfer suggest that the cooling loop pH does not appear to be sensitive to the NH_3 mass transfer coefficient, except for cases where both the makeup alkalinity and the mass transfer coefficients are low (e.g., ALK_m<90 mg/L as $CaCO_3$, and $k_{NH3}< 4\times10^{-3}$ m/s). The results also indicate that the cooling loop pH is less sensitive to the mass transfer coefficient of CO_2 at lower alkalinity levels but it can be significantly affected when CO_2 mass transfer coefficient is low (e.g., $k_{CO2}< 4\times10^{-6}$ m/s).

Analyses of the effects of cooling loop operating parameters indicate that the rates of evaporation of volatile constituents, to a large extent, are proportional to the flow rate of the blowdown stream. The impact of aqueous water chemistry appears to be significant in predicting the CO_2 evaporation rate and assuming simple water chemistry can lead to 10-15% under prediction in the range of pH expected in the cooling loop. However, NH_3 evaporation rate, over the entire range of pH can be accurately estimated using simple water chemistry.

Acknowledgments

The financial support provided by the United States Department of Energy, National Energy Technology Laboratory for this study is greatly appreciated by the authors.

Nomenclature

α: Volatile fraction of total ammonia (--)

β: Volatile fraction of carbonate (--)

A: Area for mass transfer (m^2)

a: Specific area of the cooling tower ($m^2.m^{-3}$)

A_{fr}: Frontal area of the cooling tower (m^2)

ALKm: Makeup water alkalinity

$B1_{CO2}$: Defined by equation 26 ($m^3.s^{-1}$)

$B2_{CO2}$: Defined by equation 26 ($mol.s^{-1}$)

B_{NH3}: Defined by equation 24 ($m^3.s^{-1}$)

$C_{C,L}$: Concentration of total carbonate in blowdown ($mol.m^{-3}$)

$C_{C,MU}$: Concentration of total carbonate in makeup ($mol.m^{-3}$)

$C_{i,L}$: Total concentration of component i in blowdown ($mol.m^{-3}$)

$C_{i,MU}$: Total concentration of component i in makeup water ($mol.m^{-3}$)

C_{CO2}: Concentration of CO2 in the water at the inlet of cooling tower ($mol.m^{-3}$)

$C_{CO2,air}$: Concentration of CO2 in air at the inlet of cooling tower ($mol.m^{-3}$)

C_{CO2}^*: Concentration of CO2 in water in equilibrium with the air ($mol.m^{-3}$)

$C_{N,L}$: Concentration of total ammonia in blowdown ($mol.m^{-3}$)

$C_{N,MU}$: Concentration of total ammonia in makeup ($mol.m^{-3}$)

C_{NH3}: Concentration of NH3 in the water at the inlet of cooling tower ($mol.m^{-3}$)

$C_{NH3,air}$: Concentration of NH3 in air at the inlet of cooling tower ($mol.m^{-3}$)

$C_{NH3,air}^*$: Concentration of NH3 in air in equilibrium with the water ($mol.m^{-3}$)

Cp_w: Heat capacity of water ($J.kg^{-1}.^{\circ}K^{-1}$)

F_B: Volumetric flow of blowdown stream ($m^3.s^{-1}$)

F_E: Volumetric flow of evaporation stream ($m^3.s^{-1}$)

F_{MU}: Volumetric flow of makeup stream ($m^3.s^{-1}$)

G_a: Specific mass flow of the air to the cooling tower ($kg.s^{-1}.m^{-2}$)

463 G_w: Specific mass flow of the water to the cooling tower ($kg.s^{-1}m^{-2}$)

464 $[H^+]$: Concentration of proton ion ($mol.m^{-3}$)

465 H_a: Enthalpy of humid air ($J.kg^{-1}$)

466 $H_a^{T^w}$: Enthalpy of saturated air evaluated at the water temperature ($J.kg^{-1}$)

467 K: Water evaporation mass transfer coefficient ($kg.m^{-2}.s^{-1}$)

468 $Ka1_C$: First dissociation constant of carbonic acid ($mol.m^{-3}$)

469 $(KH)_{CO2}$: CO_2 Henry's constant (--)

470 $(KH)_{NH3}$: NH_3 Henry's constant (--)

471 k_{CO2}: Overall mass transfer coefficient of CO_2 based on the water phase ($m.s^{-1}$)

472 $k_{CO2\text{-}g}$: Gas phase mass transfer coefficient of CO_2 ($m.s^{-1}$)

473 $k_{CO2\text{-}w}$: Water phase mass transfer coefficient of CO_2 ($m.s^{-1}$)

474 k_{NH3}: Overall mass transfer coefficient of NH_3 based on the gas phase ($m.s^{-1}$)

475 $k_{NH3\text{-}g}$: Gas phase mass transfer coefficient of NH_3 ($m.s^{-1}$)

476 L: Total height of the cooling tower (m)

477 L_{fz}: Height of the filling zone of the cooling tower (m)

478 m_a: Mass flow rate of air to the cooling tower ($kg.s^{-1}$)

479 M_e: Merkel number of the cooling tower (--)

480 M_{e-fz} : Merkel number of the filling zone of the cooling tower (--)

481 m_w: Mass flow rate of the water at the inlet of the cooling tower ($kg.s^{-1}$)

482 n_1, n_2, and n_3: Merkel number correlation parameters (--)

483 N_{CO2}: CO_2 evaporation rate ($kg.s^{-1}$)

484 N_{NH3}: NH_3 evaporation rate ($kg.s^{-1}$)

485 T_{avg}: Air water average temperature ($^\circ$K)

486 T^w: Water temperature ($^\circ$K)

487 T^{wi}: Water temperature at the inlet of the cooling tower ($^\circ$K)

488 T^{wo}: Water temperature at the outlet of the cooling tower ($^\circ$K)

489

References

Argonne National Laboratory, 2007. Use of Reclaimed Water for Power Plant Cooling (ANL/EVS/ R-07/3).

Bott, T. R., 1995. Fouling of Heat Exchangers (ISBN# 9780444821867). Elsevier Science & Technology Books, Birmingham, UK.

Budzianowski., W., and Koziol. A., 2005. Stripping of Ammonia from Aqueous Solutions in the Presence of Carbon Dioxide Effect of Negative Enhancement of Mass transfer. Chemical Engineering Research and Design 83(A2), 196–204.

Cabassud, C., Burgaud, C., Espenan, J.M, 2001. Spring water treatment with ultrafiltration and stripping, Desalination 137 (1-3), 123–131.

Contreras, E.M., 2007. Carbon Dioxide Stripping In Bubbled Columns. Industrial & Engineering Chemistry Research 46 (19), 6332-6337.

DOE/NETL, 2009a. Water Requirements for Existing and Emerging Thermoelectric Plant Technologies (DOE/NETL-402/080108).

DOE/NETL, 2009b. Use of Non-Traditional Water for Power Plant Applications: An Overview of DOE/NETL R&D Efforts (DOE/NETL-311/040609).

Dzombak, D. A., Vidic, R. A. and Landis, A. E. 2012. Use of TreatedMunicipal Wastewater as Power Plant Cooling System Makeup Water: TertiaryTreatment versus Expanded Chemical Regimen for Recirculating Water Quality Management. Submitted to U.S. Department of Energy, National Energy Technology Laboratory, Pittsburgh, PA.

EPRI, 2003. Use of Degraded Water Sources as Cooling Water in Power Plants (P500-03-110).

Hasson, D., Sherman, H., Biton., M., 1978. Prediction of Calcium Carbonate Scaling Rate. Proceeding of 6th international Symposium on Fresh Water from the Sea 2, 193-199.

Hasson D., Avriel, M., Resnick, W., Rozenman, T., and Windreich, S., 1968a. Calcium Carbonate Scale Deposition on Heat Transfer Surfaces. Desalination 5 (1), 107-119.

515 Hasson, D., Avriel, M., Resnick, W., Rozenman, T., and Windreich, S., 1968b. Mechanism of
516 Calcium Carbonate Scale Deposition on Heat Transfer Surfaces. Industrial & Engineering
517 Chemistry Fundamental 7 (1), 59-65.

518 Hawthorn, D., 2009. Heat Transfer: Solving Scaling Problems at the Design Stage. Chemical
519 Engineering Research and Design 87 (2), 193-199.

520 Hsieh, M.K., Walker, M.E., Safari, I., Chien, S.C., Abbasian, J., Vidic, R.V., and Dzombak,
521 D.A. 2012, Ammonia Stripping in Open-Recirculating Cooling Water Systems. Environmental
522 Progress & Sustainable Energy DOI: 10.1002/ep.11648.

523 Hsieh, M.K., Li, H., Chien, S.H., Monnell, J.D., Chowdhury, I., Dzombak, D.A., and Vidic,
524 R.V., 2010. Corrosion Control when Using Secondary Treated Municipal Wastewater as
525 Alternative Makeup Water for Cooling Tower Systems. Water Environment Research 82 (12),
526 2346-2356.

527 Kloppers, J.C., 2003 .A Critical Evaluation and Refinement of the Performance of Wet-Cooling
528 Towers. PhD Thesis, University of Stellenbosch, Stellenbosch, South Africa.

529 Kloppers, J.C., and Kröger, D., G., 2001. A Critical Cooling Tower Performance Evaluation. 12th
530 IARH Symposium in Cooling Tower and Heat Exchangers, University of Technology, Sydney,
531 Australia.

532 Kröger, D.G., 2004. Air-Cooled Heat Exchangers and Cooling Towers. Penn Well Corp. Tulsa,
533 OK.

534 Kröger, D.G., 1998. Air-Cooled Heat Exchangers and Cooling Towers Thermal-Flow
535 Performance, Evaluation and Design. Begell House Incorporate, New York, NY.

536 Li, H., Chien, S.H., Hsieh, M.K., Dzombak, D.A., and Vidic, R.D., 2011a. Escalating Water
537 Demands for Energy Production and the Potential for Use of Treated Municipal Wastewater.
538 Environmental Science & Technology 45(10), 4195-4200.

539 Li, H., Hsieh, M.K., Chien, S.H., Monnell, J.D., Dzombak, D.A., and Vidic, R.V., 2011b.
540 Control of Mineral Scale Deposition in Cooling Systems Using Secondary-Treated Municipal
541 Wastewater. Water Research 45 (2), 748-760.

542 Ma´ckowiak, J.F., Górak, A., 2011. Experimental Model Validation of an Integrated Process for
543 the Removal of Carbon Dioxide from Aqueous Ammonia Solutions, Chemical Engineering
544 Research and Design 89 (8), 1252-2160.

545 Merkel, F., 1925. Verdunstungskühlung. VDl-Zeitschrift 70, 123-128.

546 Morse, R.W., and Knudsen, J.G., 1977. Effect of Alkalinity on the Scaling of Simulated Cooling
547 Tower Water. The Canadian Journal of Chemical Engineering 55 (3), 272-278.

548 Nebot, E., Casanueva, J.F., Casanueva, T., and Sales, D., 2007. Model for Fouling Deposition on
549 Power Plant Steam Condensers Cooled with Seawater: Effect of Water Velocity and Tube
550 Material. International Journal of Heat and Mass Transfer 50 (17-18), 3351–3358.

551 Ning, R.Y., 2002. Discussion of Silica Speciation, Fouling, Control and Maximum Reduction.
552 Desalination 151 (1-2) 67-73.

553 Poppe, M., and Rögener, H., 1991. Berechnung von RückkÜhlwerken. VDI Wärmeatlas, Mi 1-
554 Mi 15.

555 Safari, I., Walker. M.E., Abbasian, J., Hsieh, M.K., Dzombak, D.A., Liu., W., Vidic, R.D, and
556 Miller, D.C., Effect of CO2 Stripping on pH in Open-Recirculating Cooling Water Systems,
557 Paper accepted for publication in Environmental Progress & Sustainable Energy, 2013 (in press).

558 Segev, R., Hasson, D., and Semiat, R., 2012. Rigorous Modeling of the Kinetics of Calcium
559 Carbonate Deposit Formation. AIChE Journal 58 (7), 2286-2289.

560 Sander, R. 1999. Compilation of Henry's Law Constants for Inorganic and Organic Species of
561 Potential Importance in Environmental Chemistry, Air Chemistry Department Max-Planck
562 Institute of Chemistry, Mainz, Germany.

563 Sherwood., T.K., Draemel, F.C., and Rukman N.E. 1937. Desorption of Carbon Dioxide from
564 Water in a Packed Tower, Industrial and Engineering Chemistry 29 (3), 282-285.

565 Sultan, K.M., Zubair, S.M, Budair, M.O., Sheikh, A.K., and Quddus, A., 1996. Fouling
566 Resistance Model for Prediction of CaCO3 Scaling in AISI 316 Tubes. Heat and Mass Transfer
567 Springer-Verlag 32 (1-2), 73-79.

568 Taborek, J., Aoki, T., Ritter, R.B., Palen, J.W., and Kundsen, J.G., 1972a. Fouling: The Major
569 Unresolved Problem in Heat Transfer. Chemical Engineering Progress 68 (2), 59-67.

570 Taborek, J., Aoki, T., Ritter, R.B., Palen, J.W., and Knudsen, J.G., 1972b. Predictive Methods
571 for Fouling Behavior. Chemical Engineering Progress 68 (7), 69-78.

572 USGAO, 2003. Freshwater Supply—States' Views of How Federal Agencies Could Help Them
573 Meet the Challenges of Expected Shortages, (GAO-03-514). U.S. General Accounting Office,
574 Washington, DC.

575 USGS, 2009. Estimated Use of Water in the United States in 2005 (USGS Circular 1344). U.S.
576 Geological Survey, Reston, VA.

577 USGS, 1998. Estimated Use of Water in the United States in 1995 (USGS Circular 1200). U.S.
578 Geological Survey, Reston, VA.

579 Vidic, R.V., and Dzombak, D.A., 2009. Reuse of Treated Internal or External Wastewaters in the
580 Cooling Systems of Coal-based Thermoelectric Power Plants (DE-FC26-06NT42722).
581 Submitted to U.S. Department of Energy, National Energy Technology Laboratory, Pittsburgh,
582 PA.

583 Walker, M.E., Safari, I., Theregowda, R.B., Hsieh, M.K., Abbasian, J., Arastoopour, H.,
584 Dzombak, D.A., and Miller D.C., 2012, Economic impact of condenser fouling in existing
585 thermoelectric power plants, Energy, 44 (1), 429–437.

586 Wiechers, H.N.S., Sturrock, P., and Marais, G.V.R., 1975. Calcium Carbonate Crystallization
587 Kinetics. Water Research 9.(9), 835-845.

588 Williamson, N.J., 2008. Numerical Modeling of Heat and Mass Transfer and Optimization of a
589 Natural Draft Wet Cooling Tower, PhD Thesis, the School of Aerospace, Mechanical and
590 Mechatronic Engineering, The University of Sydney, Australia.

591 Yoon, H., Lim, J.H., and Chung, H.K, 2008. Ammonia Removal Model Based on the
592 Equilibrium and Mass Transfer Principles, Bulletin Korean Chemical Society 29 (3), 555-561.

List of Tables

List of Figures

Figure 10: a-Effect of condenser heat load on the cooling loop pH when temperatures remain at base case condition for MWW. b- Effect of condenser heat load on the cooling loop pH when the recirculating water flow rate remains at base case condition for MWW. c- Effect of cooling tower inlet water temperature for MWW.

Figure 11: a- Volatile fraction of total ammonia and carbonate from Aspen/OLI water chemistry and simplified water chemistry. b- Evaporation rates predicted by Aspen/OLI water chemistry and simplified water chemistry

Table 1

Parameter	Value
Makeup water temperature, ºC	25
Water inlet temperature to the cooling tower, ºC	40 to 45
Water outlet temperature from cooling tower, ºC	25 to 35
Inlet air temperature (dry bulb), ºC	28
Inlet air relative humidity, %	60
Cooling tower filling height, m	0.915
Gas-liquid interfacial area, $m^2.m^{-3}$	147.5
Cycles of concentrations	2 to 10
Condenser heat duty, kJ/S	811085
Merkel number parameters of equation 4 (Kröger, 2004):	
n_1	0.279
n_2	-0.094
n_3	0.602

Table 2

Analyses	Unit	MWW[a]	MWW-N[b]
Al	mg/L	0.2	0.2
Ca	mg/L	41.5	41.5
Fe	mg/L	0.504	0.504
K	mg/L	16.3	16.3
Mg	mg/L	10.7	10.7
Mn	mg/L	0.317	0.317
Na	mg/L	94.2	94.2
SiO_2	mg/L	8.54	8.54
pH		7.1	6.7
NH3-N	mg/L	21.0	0.05
Bicarbonate Alkalinity	mg/L as $CaCO_3$	177	25.0
Cl	mg/L	106	106
NO3-N	mg/L	3.6	18.1
SO_4	mg/L	86	86
Total P	mg/L	4.5	4.5

[a]: Samples from Franklin Township Municipal Sanitary Authority September 2008 (Vidic & Dzombak, D.A., 2009)

[b]: Simulation results for tertiary treatment of MWW with nitrification

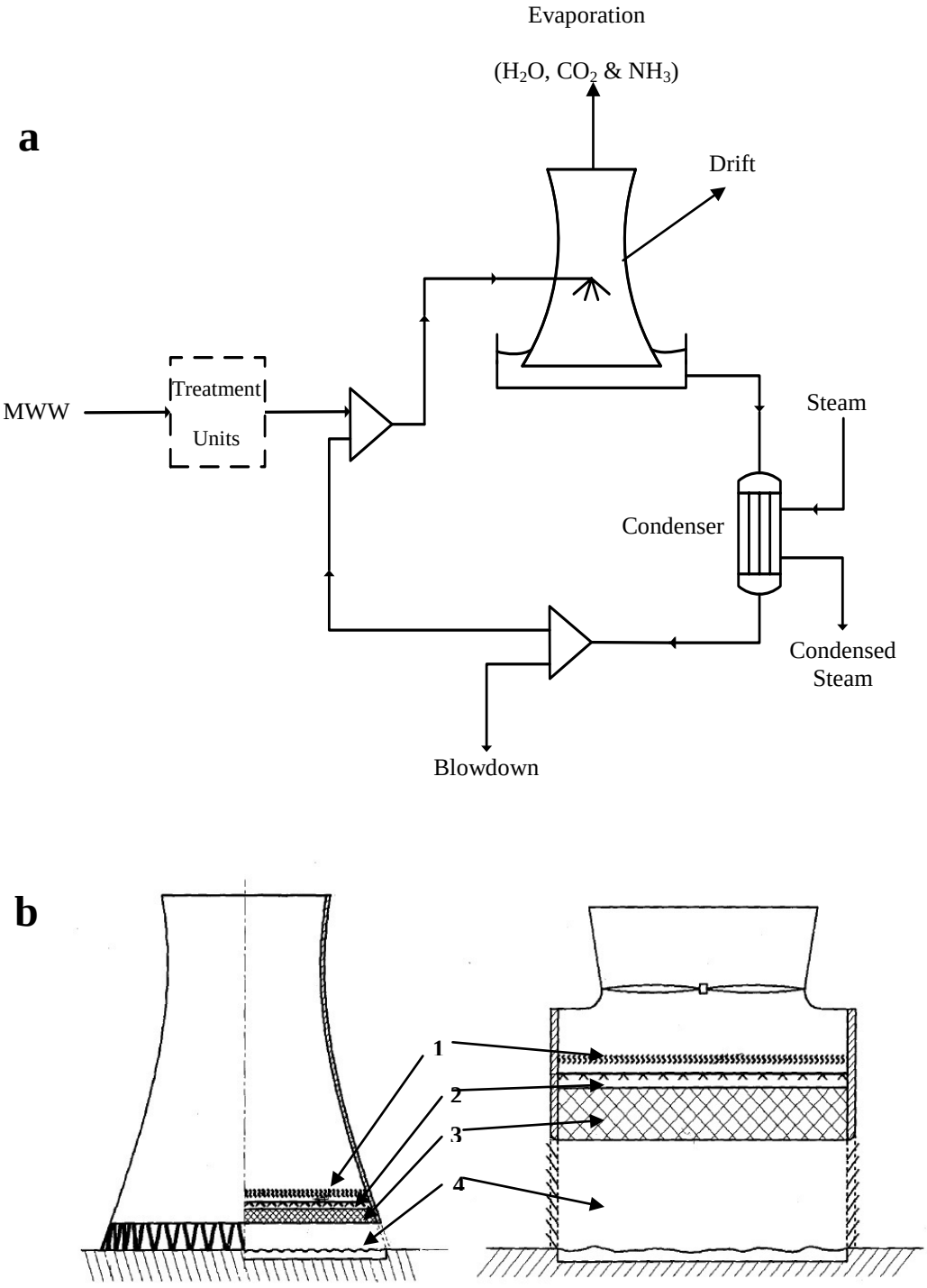
a
Evaporation
(H_2O, CO_2 & NH_3)
Drift
MWW
Treatment
Units
Steam
Condenser
Condensed
Steam
Blowdown
b
1
2
3
4

Figure 1

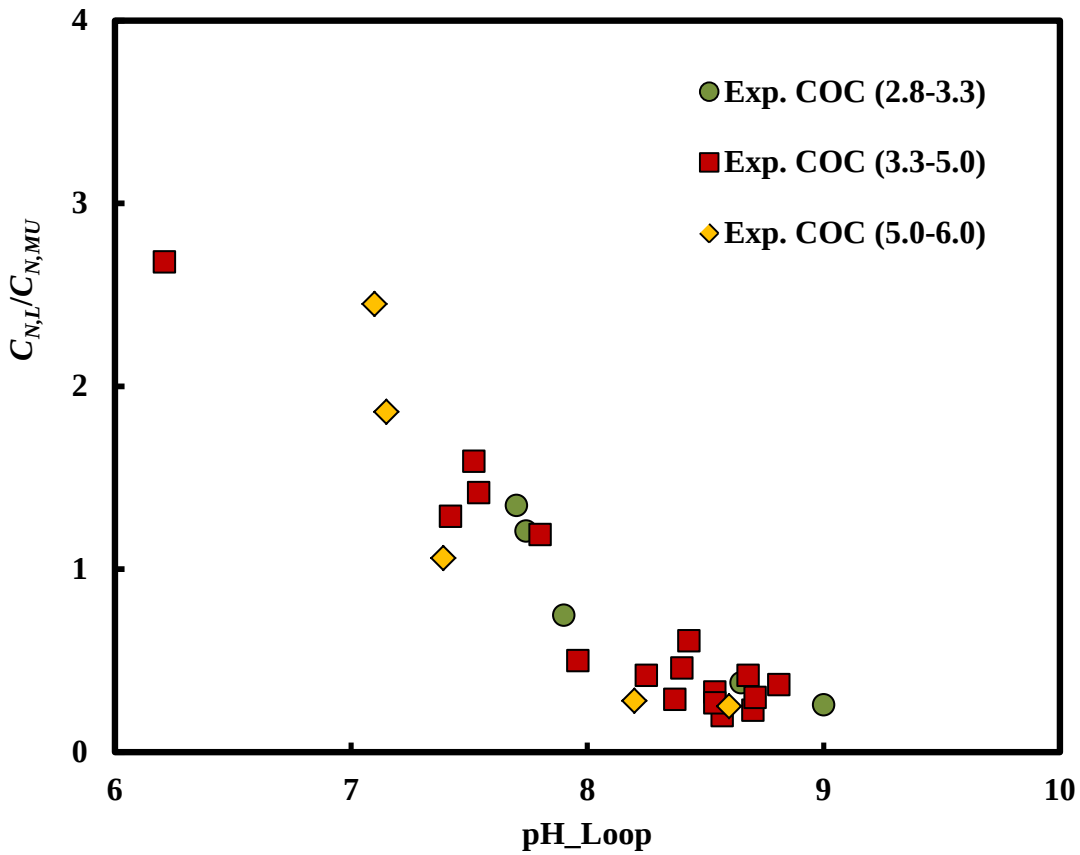
Exp. COC (2.8-3.3)
Exp. COC (3.3-5.0)
Exp. COC (5.0-6.0)
$C_{N,L}/C_{N,MU}$
pH_Loop
0
1
2
3
4
6
7
8
9
10

Figure 2

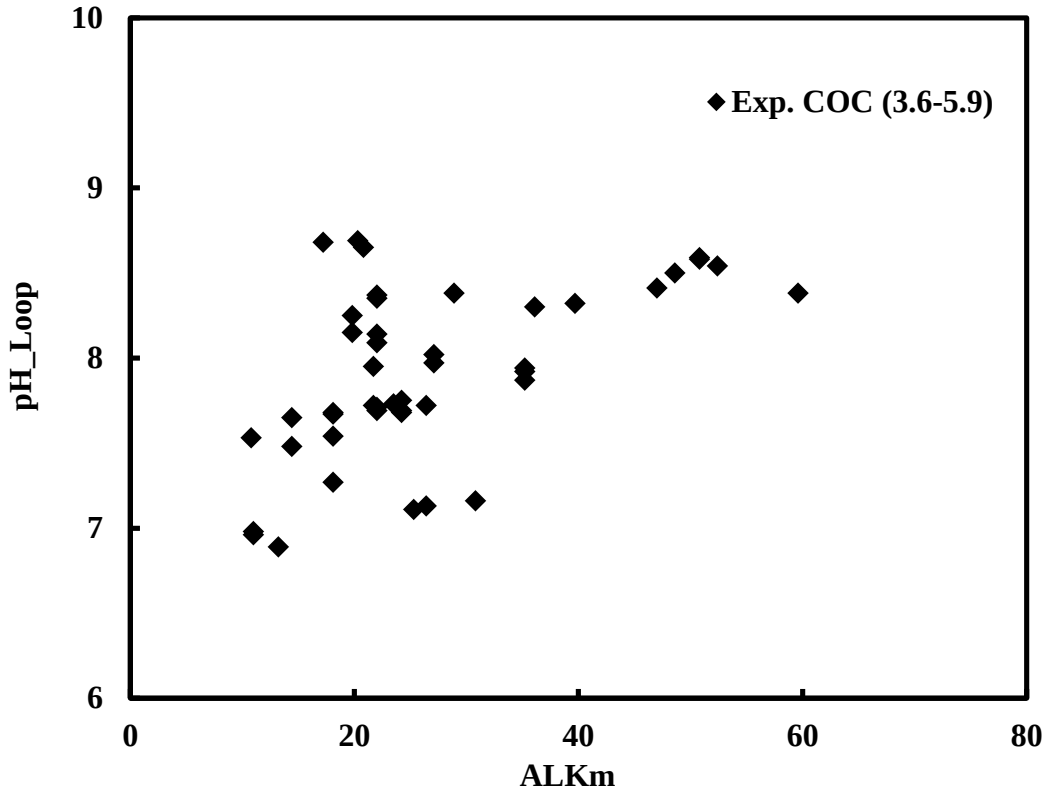

Figure 3

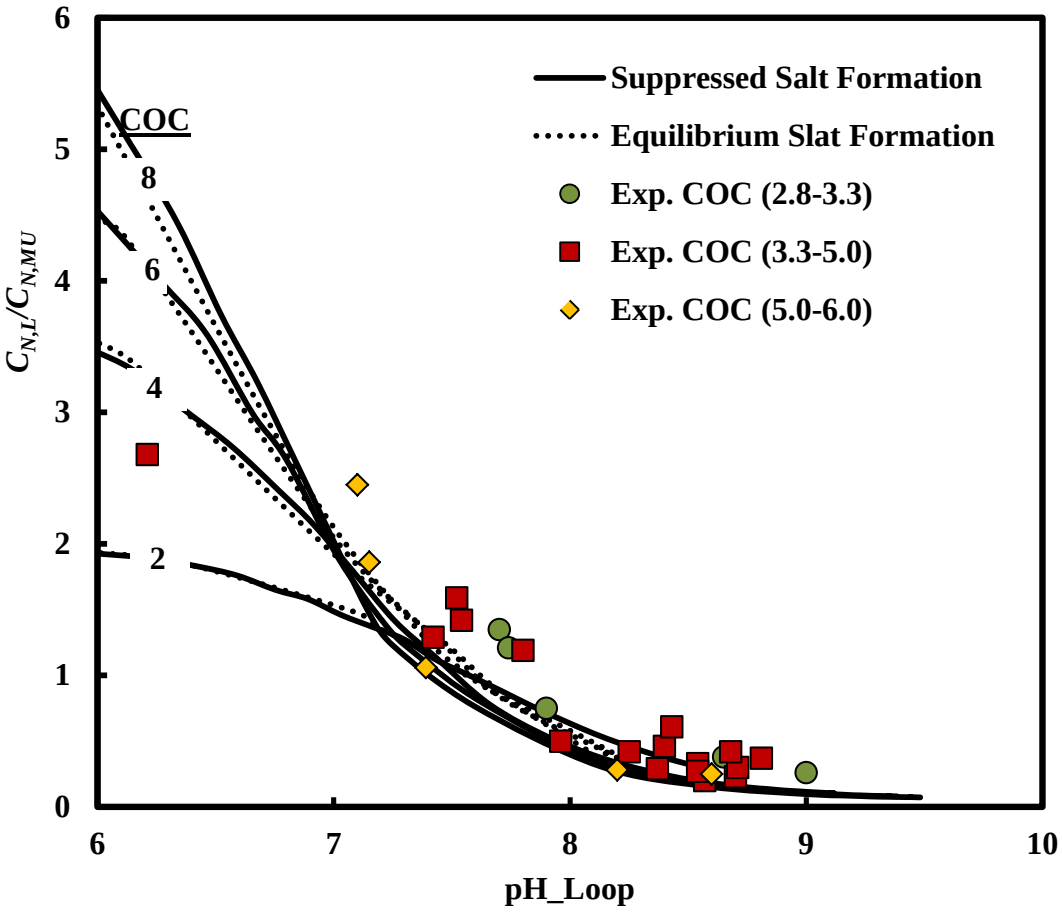
Suppressed Salt Formation
Equilibrium Slat Formation
Exp. COC (2.8-3.3)
Exp. COC (3.3-5.0)
Exp. COC (5.0-6.0)
COC
8
6
4
2
$C_{N,L}/C_{N,MU}$
pH_Loop
0
1
2
3
4
5
6
6
7
8
9
10

Figure 4

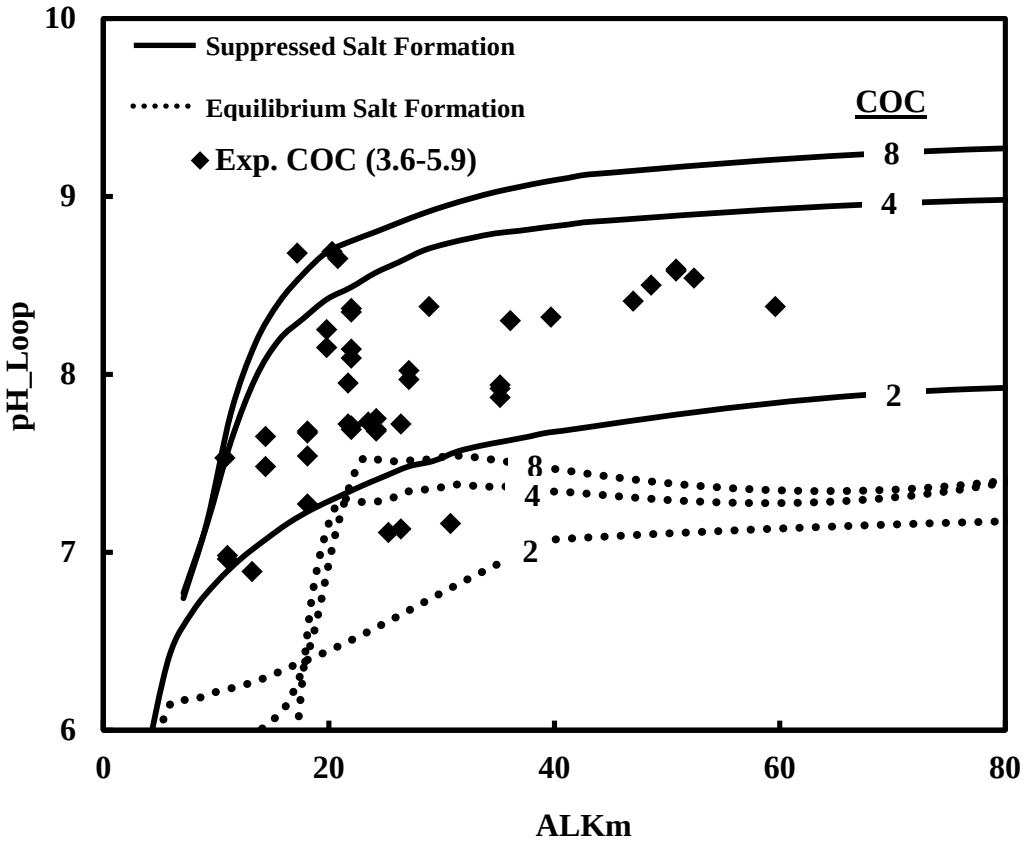
Suppressed Salt Formation
Equilibrium Salt Formation
Exp. COC (3.6-5.9)
COC
8
4
2
8
4
2
pH_Loop
ALKm
10
9
8
7
6
0
20
40
60
80

Figure 5

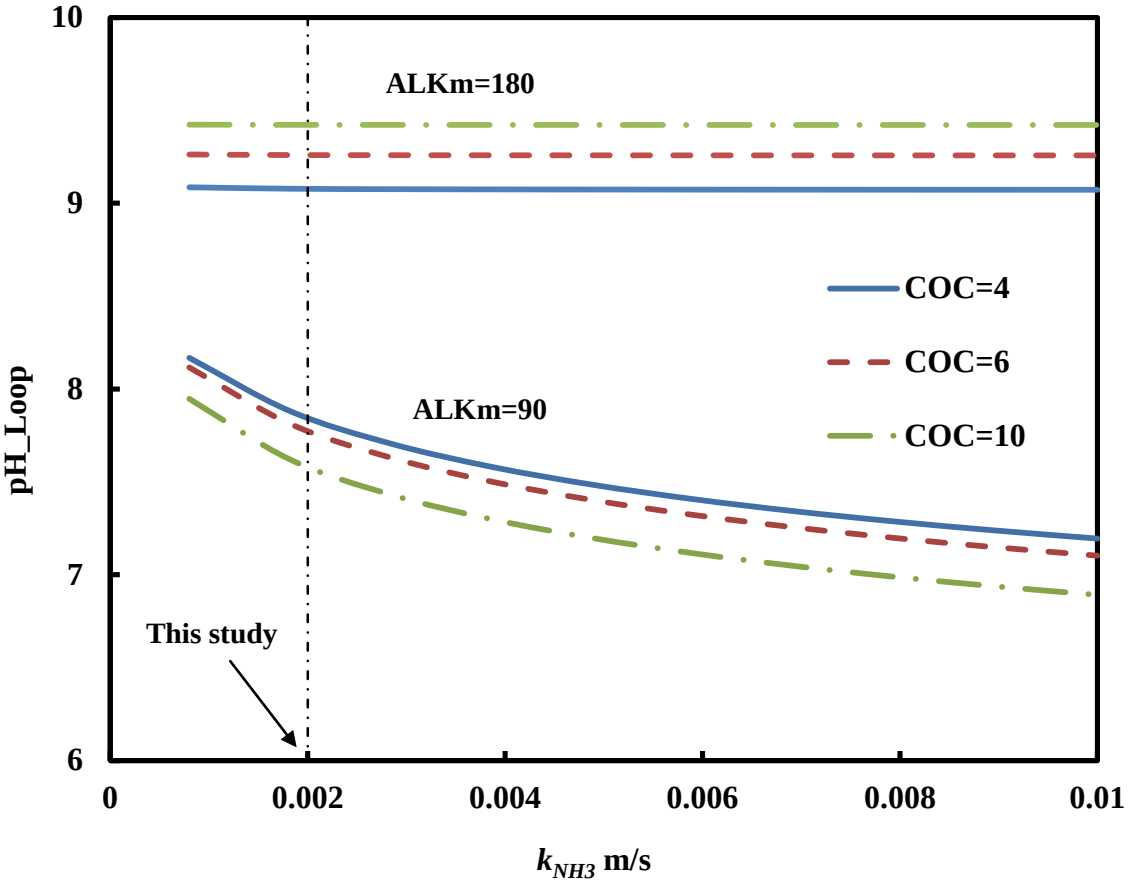
10
9
8
7
6
pH_Loop
ALKm=180
ALKm=90
COC=4
COC=6
COC=10
This study
0
0.002
0.004
0.006
0.008
0.01
k_{NH3} m/s

Figure 6

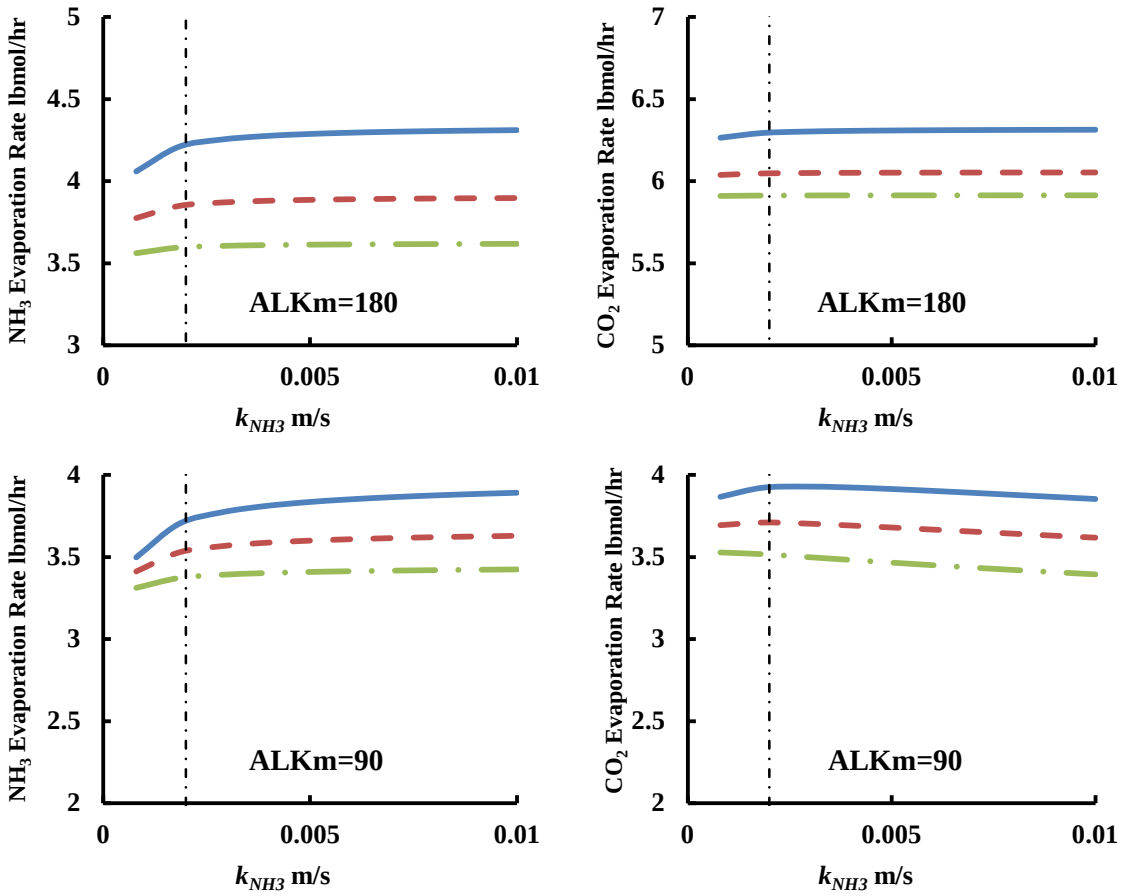
NH3 Evaporation Rate lbmol/hr
CO2 Evaporation Rate lbmol/hr
ALKm=180
ALKm=90
k_NH3 m/s
0
0.005
0.01

Figure 7

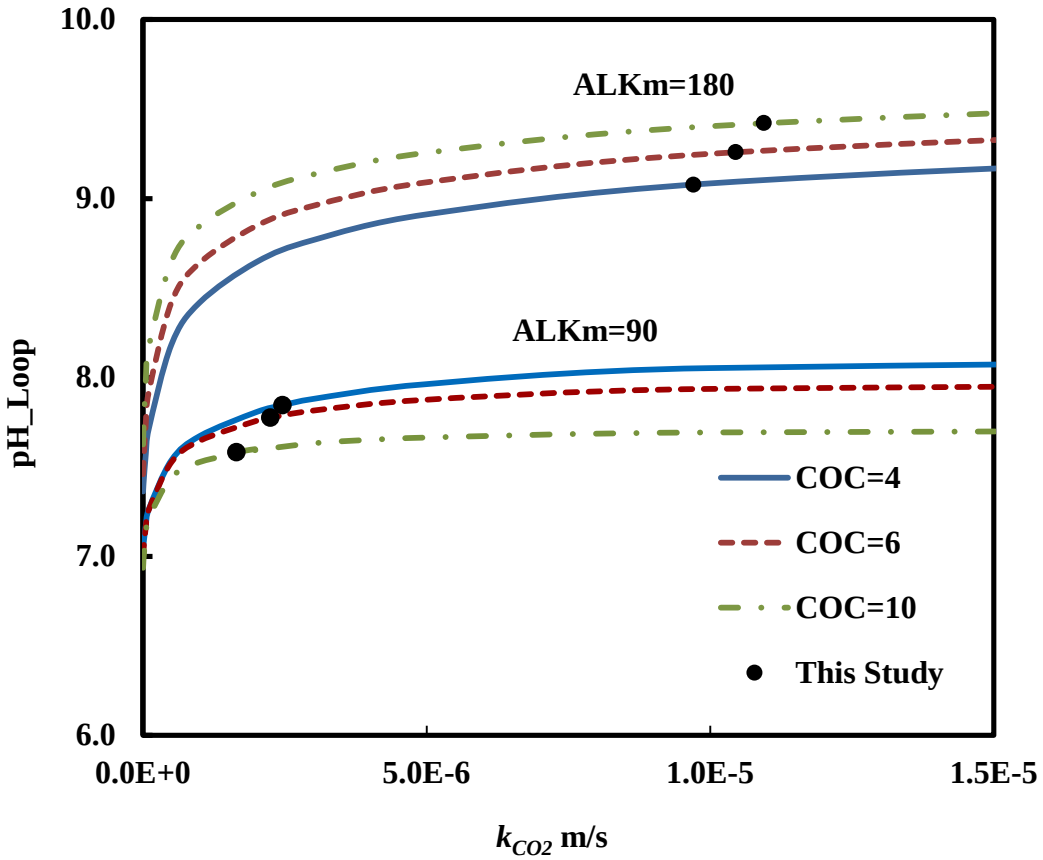
10.0
9.0
8.0
7.0
6.0
pH_Loop
ALKm=180
ALKm=90
COC=4
COC=6
COC=10
This Study
0.0E+0
5.0E-6
1.0E-5
1.5E-5
k_{CO2} m/s

Figure 8

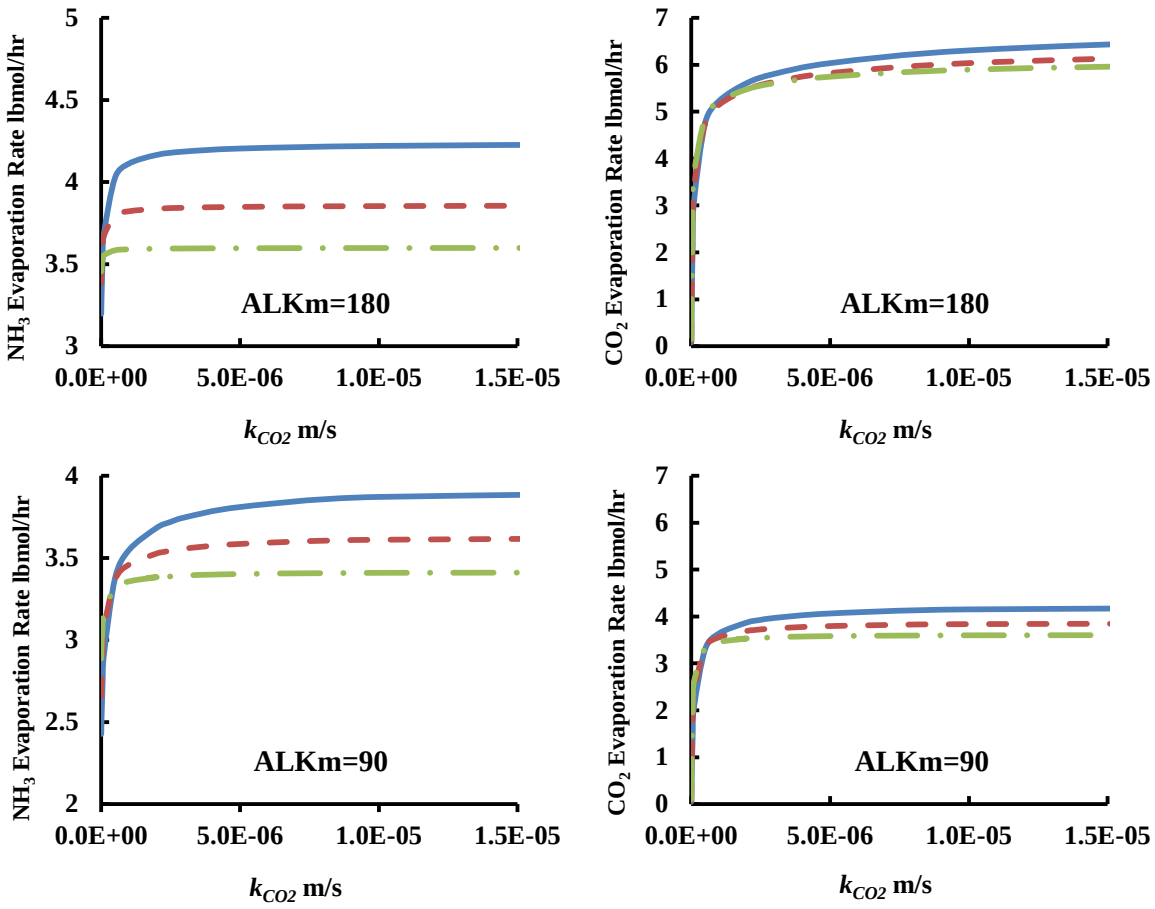
NH3 Evaporation Rate lbmol/hr
5
4.5
4
3.5
3
ALKm=180
0.0E+00
5.0E-06
1.0E-05
1.5E-05
kCO2 m/s
CO2 Evaporation Rate lbmol/hr
7
6
5
4
3
2
1
0
ALKm=180
0.0E+00
5.0E-06
1.0E-05
1.5E-05
kCO2 m/s
NH3 Evaporation Rate lbmol/hr
4
3.5
3
2.5
2
ALKm=90
0.0E+00
5.0E-06
1.0E-05
1.5E-05
kCO2 m/s
CO2 Evaporation Rate lbmol/hr
7
6
5
4
3
2
1
0
ALKm=90
0.0E+00
5.0E-06
1.0E-05
1.5E-05
kCO2 m/s

Figure 9

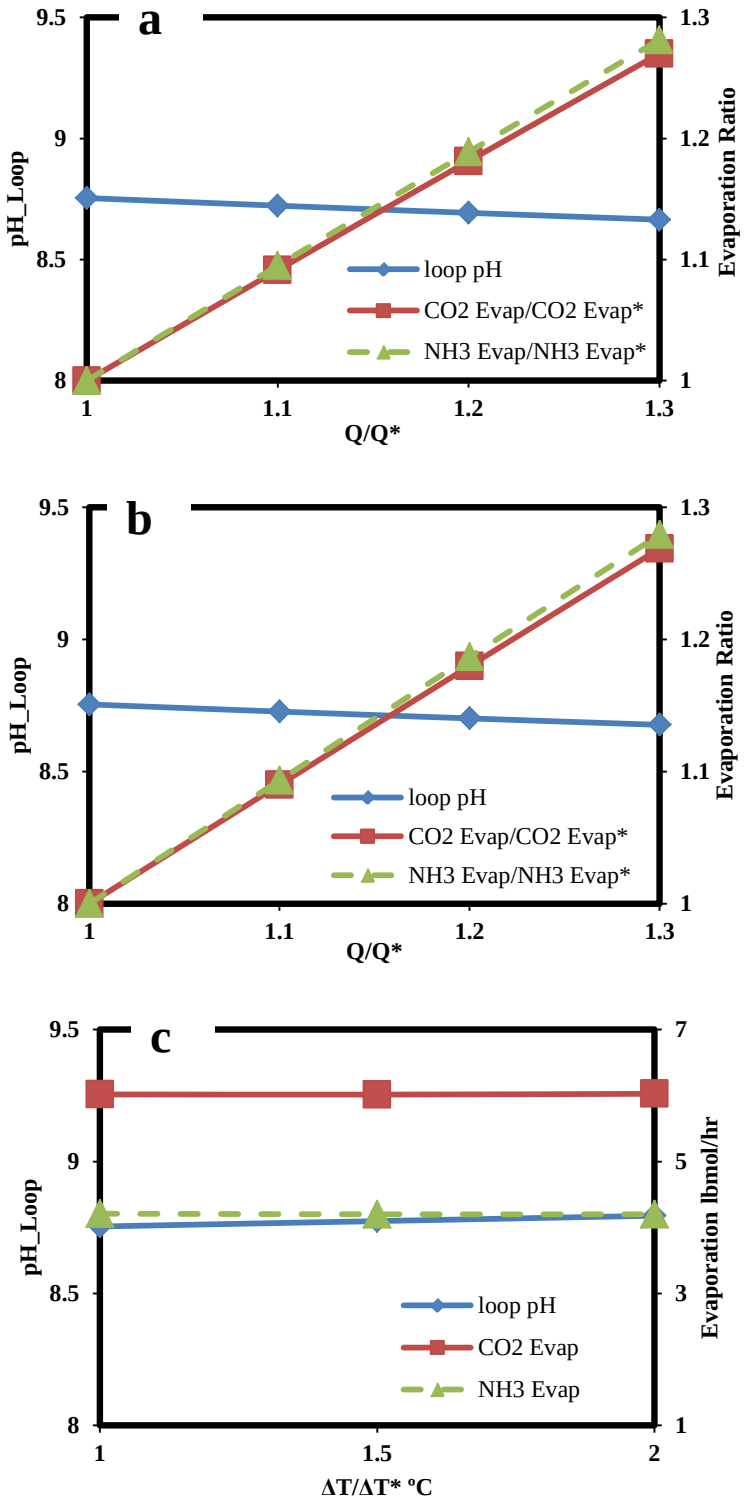
a
9.5
9
8.5
8
1.3
1.2
1.1
1
pH_Loop
Evaporation Ratio
loop pH
CO2 Evap/CO2 Evap*
NH3 Evap/NH3 Evap*
1
1.1
1.2
1.3
Q/Q*
b
9.5
9
8.5
8
1.3
1.2
1.1
1
pH_Loop
Evaporation Ratio
loop pH
CO2 Evap/CO2 Evap*
NH3 Evap/NH3 Evap*
1
1.1
1.2
1.3
Q/Q*
c
9.5
9
8.5
8
7
5
3
1
pH_Loop
Evaporation lbmol/hr
loop pH
CO2 Evap
NH3 Evap
1
1.5
2
ΔT/ΔT* °C

Figure 10

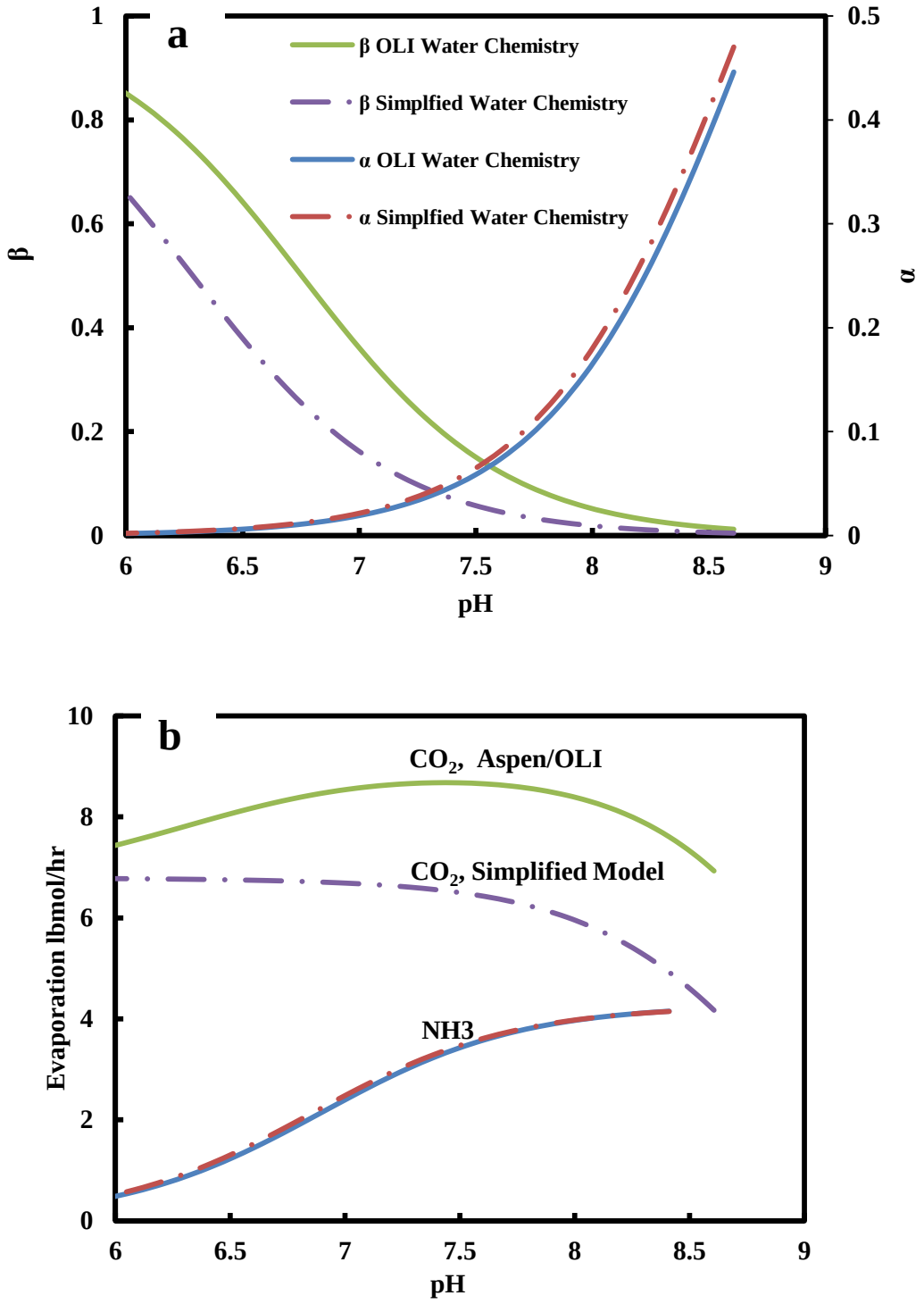
a
β OLI Water Chemistry
β Simplfied Water Chemistry
α OLI Water Chemistry
α Simplfied Water Chemistry
β
α
pH
1
0.8
0.6
0.4
0.2
0
0.5
0.4
0.3
0.2
0.1
0
6
6.5
7
7.5
8
8.5
9
b
CO2, Aspen/OLI
CO2, Simplified Model
NH3
Evaporation lbmol/hr
pH
10
8
6
4
2
0

Figure 11